5th ECPMG Delft · 2024

Proceedings of the 5th ECPMG 2024
5th European Conference on Physical Modelling in Geotechnics
2-4 October 2024, Delft, the Netherlands

Increasing the Confinement in Railway Track Ballast Layers

Stanislav Lenart
Slovenian National Building and Civil Engineering Institute (ZAG), Ljubljana, Slovenia, stanislav.laenart@zag.si

Siva Ram Karumanchi
Slovenian National Building and Civil Engineering Institute (ZAG), Ljubljana, Slovenia, ram.karumanchi@zag.si

ABSTRACT: Insufficient effective confining pressure within the ballast layer can lead to the permanent rotation of grains, causing increased wear and abrasion. Augmenting confinement may not only mitigate ballast degradation but also enhance the overall performance of the track. The increased confining pressure causes the increase of ballasted track stiffness and reduction of resilient and permanent deformation. This paper outlines developing a cost-effective ballast wall arrangement (BWA) to boost ballast layer confinement without disrupting maintenance procedures. It involves incorporating specific secondary raw material elements along the track shoulder, combined with a horizontal geosynthetic reinforcing layer at the base of the ballast layer. These shoulder elements not only impact the track's geometry but also facilitate a reduction in required ballast volume. The efficacy of the ballast confinement mechanism has undergone small-scale testing to prove the concept of reinforcement. Numerical modeling has been developed, which plays a crucial role in supporting the optimal design of this solution.
Keywords: ballast, railway track, geosynthetics, confining pressure, small-scale test

1 BACKGROUND

Railway infrastructure commonly relies on ballasted tracks, playing a crucial role with three key functions: i) uniformly transmitting the trainload to the underlying subgrade, ii) upholding track geometry and alignment, and iii) functioning as a drainage barrier. Ballasted tracks are most commonly used for railway infrastructure. The primary drawbacks of ballasted tracks are linked to track stability, arising from the gradual degradation of the ballast over time, leading to excessive vertical and lateral settlements (Sadeghi and Askarinejad, 2009). This causes ballast aggregates to spread laterally due to inadequate confining pressure, misalignment, and, ultimately, train derailments. Moreover, the fines produced during particle breakage and degradation contribute to void filling, ultimately reducing the drainage capacity of the ballast material (Prasad and Hussaini, 2022). After a certain operational timeframe, deteriorated ballast reaches a point where it is no longer viable and necessitates replenishment with newly quarried ballast. Over the past three decades, the preferred choice for ballast material has been igneous or metamorphic rocks, such as granite, given their superior performance compared to less resilient sedimentary rocks. However, countries like Slovenia, Croatia, and the Netherlands face challenges due to the limited availability of quality ballast material, leading them to resort to the utilization of sedimentary rocks with lower abrasion resistance (Guo et al., 2022). Consequently, there is a growing demand to explore innovative solutions in order to uphold track stability and reduce maintenance costs. Recently, there has been an increasing trend to conserve high-quality raw materials by incorporating secondary or waste materials. Numerous research endeavors (Indraratna, Sun and Grant, 2017; Indraratna et al., 2022; Prasad and Hussaini, 2022) have been undertaken to explore diverse and innovative approaches for leveraging recycled industrial wastes, including tire derivatives, coal wash, plastics, glass, etc., aiming to mitigate track degradation and elevate overall performance. These studies suggest that incorporating rubber granules in ballast consistently increased its performance. The findings of the laboratory experiments, which included small-scale physical tests, direct shear tests, and triaxial tests, illustrate improved dynamic properties of the modified ballast material. Notably, adding waste tire chips reduces particle breakage compared to pure ballast (Sol-Sánchez, Moreno-Navarro, and Rubio-Gámez, 2014; Gong et al., 2019). However, certain geotechnical characteristics, such as the friction angle and dilation angle, experience a slight decrease, while others, such as modulus degradation, demonstrate improvement. Despite the increase in specific dynamic properties and a reduction in particle breakage, reducing certain

geotechnical properties of the modified ballast material exacerbates confinement issues on the tracks.

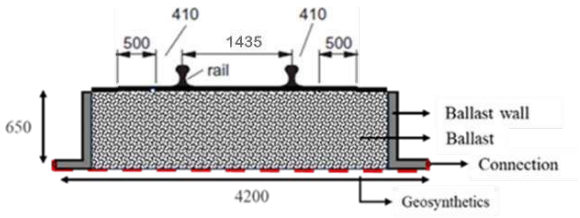

Figure 1. Illustration of an assumed field Ballast wall arrangement (dimensions in mm)

In light of this perspective, it is imperative to employ effective ground improvement techniques to enhance the confinement of both modified and pure ballast material. Enhancing the performance of granular media in road and railway infrastructure can be effectively achieved through the application of geosynthetics (Leshchinsky and Ling, 2013; Indraratna, Biabani and Nimbalkar, 2015; Biabani, Ngo and Indraratna, 2016). Several applications involving planar geosynthetics, such as geogrids, geotextiles, and geocomposites, have been employed to reduce excessive settlement and lateral displacement of tracks under cyclic loading (Indraratna, Ngo and Rujikiatkamjorn, 2013). In addition, geocell reinforcement in ballast layers has been attributed to enhanced apparent cohesion and increased confinement of ballast (Indraratna, Biabani and Nimbalkar, 2015). Similarly, ballast layer modifications, which integrate a rubber tire assembly in the load-bearing substructure and tire arc segments along the track shoulders, increased the ballast layer's confinement and minimized settlements and lateral displacements (Indraratna et al., 2022). Recently, retaining walls for ballast confinement has become more prevalent, particularly in areas with sharp curves and bridges (Aela, Jia, and Jing, 2021). This approach has demonstrated a decrease in the lateral displacement of the ballast layer. Despite these advancements, there needs to be more focus on evaluating the performance of ballast walls in the context of ballasted railway tracks. Though employing concrete walls for ballast confinement may incur higher costs than conventional ballast layer reinforcement methods, the specific advantages lie in their increased confinement, minimal space occupancy, high lateral strength, and lower railway track maintenance expenses. This study focuses on developing a unique solution that integrates low-height ballast walls with planar geogrids, depicted in Fig. 1, to effectively handle confinement issues and lateral displacements in railway tracks. Given this, a small-scale laboratory apparatus was employed to examine the lateral displacements of a confined ballast arrangement. Concurrently, a finite element model has been developed and validated, ready to optimize various parameters.

2 DESCRIPTION OF CONFINED BALLAST MECHANISM

Developed within the European project LIAISON - HORIZON-CL5-2022-D6-02-06 framework, the sustainable and low-maintenance ballast wall arrangement (referred to as BWA) in conjunction with geogrids serves as a solution. In this project, exploring all shapes, including L-shaped and T-shaped configurations, vertical wall arrangements, geogrid connections, and using rubber as ballast material, is underway to derive an optimized solution for implementation in a track section in Slovenia. The primary aim of this study is to evaluate the stability against lateral displacements in ballasted tracks by applying the BWA in conjunction with geogrids. The study proposes the sustainable inclusion of geogrids in the ballast layer to enhance the shear strength of ballasted tracks. In selecting a suitable BWA, the study considers various factors such as cost, safety, geogrid stiffness, foundation conditions, maintenance, and appearance. This paper, in particular, presents research on L-shaped ballast walls, analyzing their capability to provide sufficient stability and confinement. Following the definition of stability, the potential overturning, sliding, and bearing capacity of retaining walls are depicted in Fig 2(a) & (b). The research incorporates a series of load tests conducted under different ballast layer conditions to examine the lateral resistance of BWA.

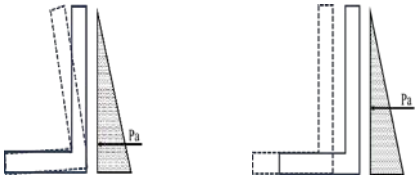

Figure 2. Stability requirements of BWA (a) Overturning (b) Sliding

3 SCALING OF MATERIALS AND SMALL-SCALE EXPERIMENTAL SETUP

Reduced-scale model tests were conducted using a test setup developed at ZAG, Ljubljana. The setup was designed to accommodate the ballast track scaled to 8. On the front side of the setup, a thick plexiglass sheet was installed to visualize the corresponding displacements from the applied load. The overall

dimensions of the setup are 250x800x200 (height, mm x length, mm x width, mm), as illustrated in Fig. 3. Moreover, in reduced model tests, scale effects are indeed critical, and their role in geotechnical model tests (1g and centrifuge model tests) has been documented by Wood (2004). Accordingly, the setup length was adjusted to 800mm to prevent boundary effects. In reduced model tests, the dry gravel samples of particle size 4-8mm obtained from the Sava river basin were used to represent 30-50mm particle size in the field scale. Fig. 4(a) & (b) presents representative sieve analysis data of field ballast (EN 13450) and dry gravel material scaled to particle size 4-8mm. The gravel samples underwent oven and air-drying to ensure dryness before preparing the test specimens. The foundation soil was prepared under dense conditions for considerable rigidity. The end-to-end reinforcement was connected to the L-shaped walls with small pins to ensure connectivity. Using the rainfall technique, the test specimens were arranged as a layered system with a known quantity of dry gravel layered at a 40mm thickness. Maintaining falling height and compaction effort ensured a desired 2 g/cm3 density. The L-shaped BWA (LSBWA) with scaled reinforcement material of lesser stiffness was initially prepared based on testing requirements. The testing program included two model tests, LSBWA 1 and LSBWA 2. Fig. 5(a) shows the first model test on LSBWA made of dry gravel with scaled railway embankment dimensions 125x500x200 (height, mm x length, mm x width, mm). LSBWA 2, shown in Fig. 6(a), was conducted with a reduced length of 350m (representing the BWA near the sleepers). The length of the connected reinforcement was ensured to be long and stiff enough to support the BWA. The model underwent a maximum scaled load of 13kN, considering Wood (2004) scaling laws (representing an 80tonne train axle load). Digital images were captured at regular intervals during testing to visualize the BWA lateral deformation path and corresponding reinforcement strains from the strain gauge placed at the center.

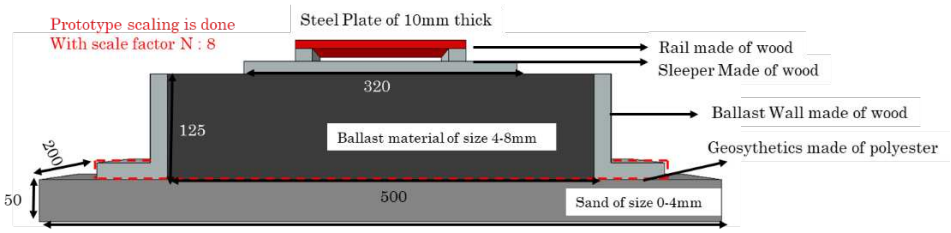

Figure 3. Illustration of the test setup (dimensions in mm)

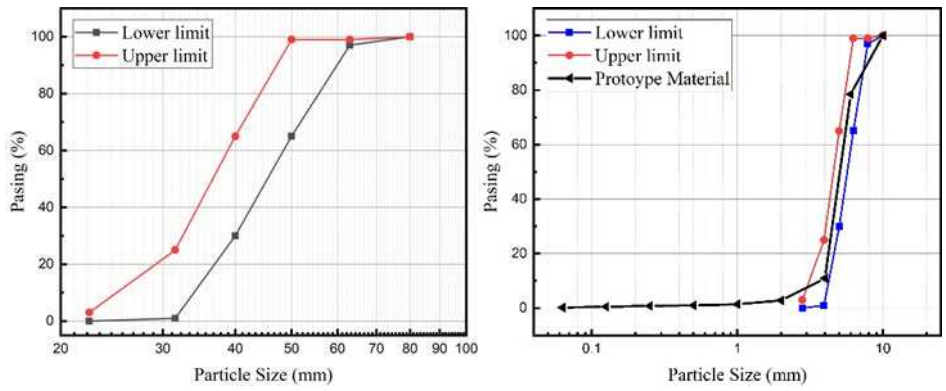

(a) (b)

Figure 4. Ballast material size chart (a) Field Ballast Curve chart (b) Prototype Ballast Curve chart (scaled to N=8)

4 MODEL TEST MEASUREMENTS

The presentations here include load application details and corresponding lateral deformation mechanisms for LSBWAs Figs. 5 & 6. The lateral displacement pattern of BWA is obtained from indicative markers in the processed image, as shown in Fig. 5(b) & 6(b). Reinforcement strains and lateral displacements are measured from strain gauges and digital images captured at various applied loads, as illustrated in Figs. 5 & 6. This study investigates lateral deformations for the BWA with end-to-end connected reinforcement. Investigations are presented to evaluate the role of reinforcement in holding the BWA against external loads. The end-to-

end reinforcement plays a role in restricting the probable overturning and sliding of the BWA. Fig. 5(c) presents complete loading and unloading data along with corresponding strains of reinforcement and lateral displacements of LSBWA 1. The influence of reinforcement and the L-shaped wall is described in Fig. 5(d) & (e), showing the strains and lateral displacement profiles of the scaled LSBWA. The maximum lateral displacement at the right and left walls of LSBWA 1 was 3 and 2.4 mm, respectively. The estimated peak strain for LSBWA-1 is 0.20% at the peak load of 13 kN. Test LSBWA 2 is performed to analyze the impact of the lesser length of ballast layers on the lateral deformation behavior of BWA. Fig. 6(c) illustrates complete loading and unloading data and corresponding strains of reinforcement and lateral displacements of LSBWA 2. The influence of reinforcement and the L-shaped wall is described in Figs. 6(d) & (e), showing the strains and lateral displacement profiles of the scaled LSBWA. The maximum lateral displacement at the right and left walls of LSBWA 2 was 5.46 and 4 mm, respectively. The estimated peak strain for LSBWA 2 is 0.35% at the peak load of 13 kN. Displacements are in the same range for both tests' left and right walls, indicating a stable condition where both walls deform similarly. Additionally, the stiffness of end-to-end connected reinforcement governs the lateral movement of the wall. As the testing process is in the initial stage of the LIAISON project, the permanent displacements due to accumulated strains from load cycles are not presented here. The lateral displacements of the BWA in both tests remain constant during the unloading case, as observed in Figs. 5 and 6. This indicates that at higher loads, ballast rearrangement occurs which was observed during the testing process, reflecting permanent lateral deformation of BWA. The stability of LSBWA is governed by the stiffness of BWA, reinforcement, and the connection between the reinforcement and BWA, which will be further studied.

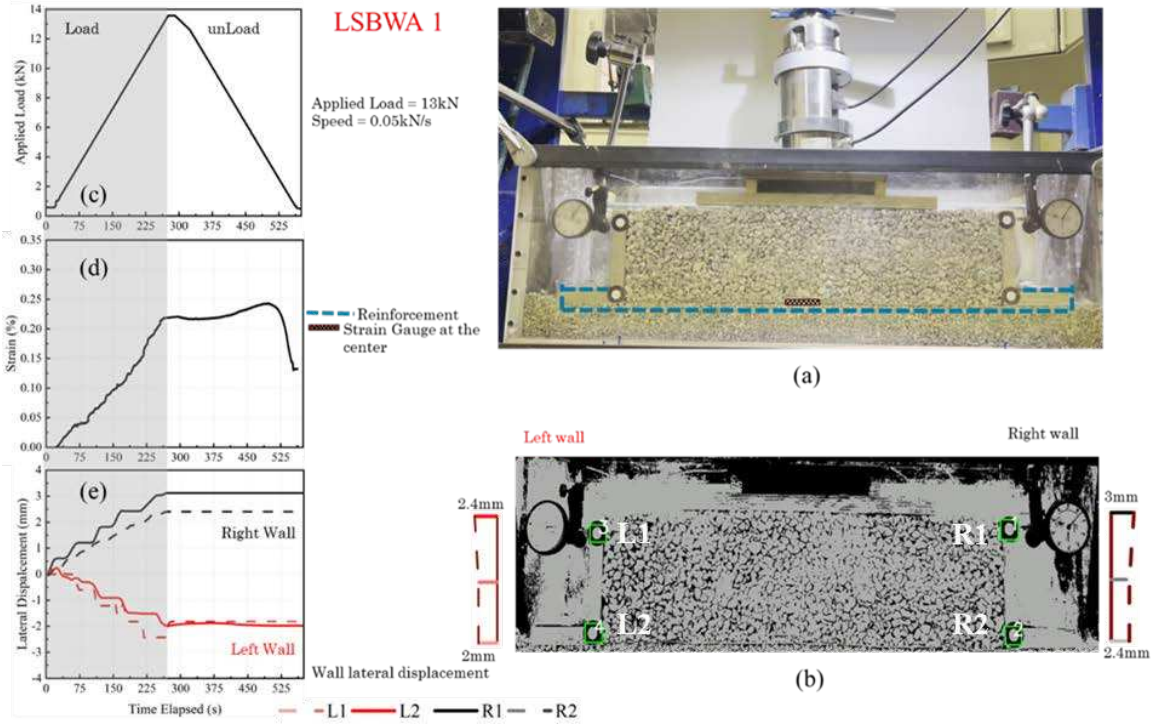

Figure 5. Test results of LSBWA 1 (a) Digital image during testing (b) Processed image (c) Loading data (d) Strain, % vs. Time elapsed, secs (e) Lateral displacement, mm vs. Time elapsed, seconds

Table 1. Material Properties used in the Numerical model

Description	Density	E,	Poisson's ratio	Peak Angle of Internal Friction	Dilation Angle	Cohesion
	Ton/m3	kPa				kPa
Gravel	2	20000	0.3	50	5	0
Sand	1.7	2500	0.3	38	8	0
Reinforcement	0.9	2000	0.15	-	-	-

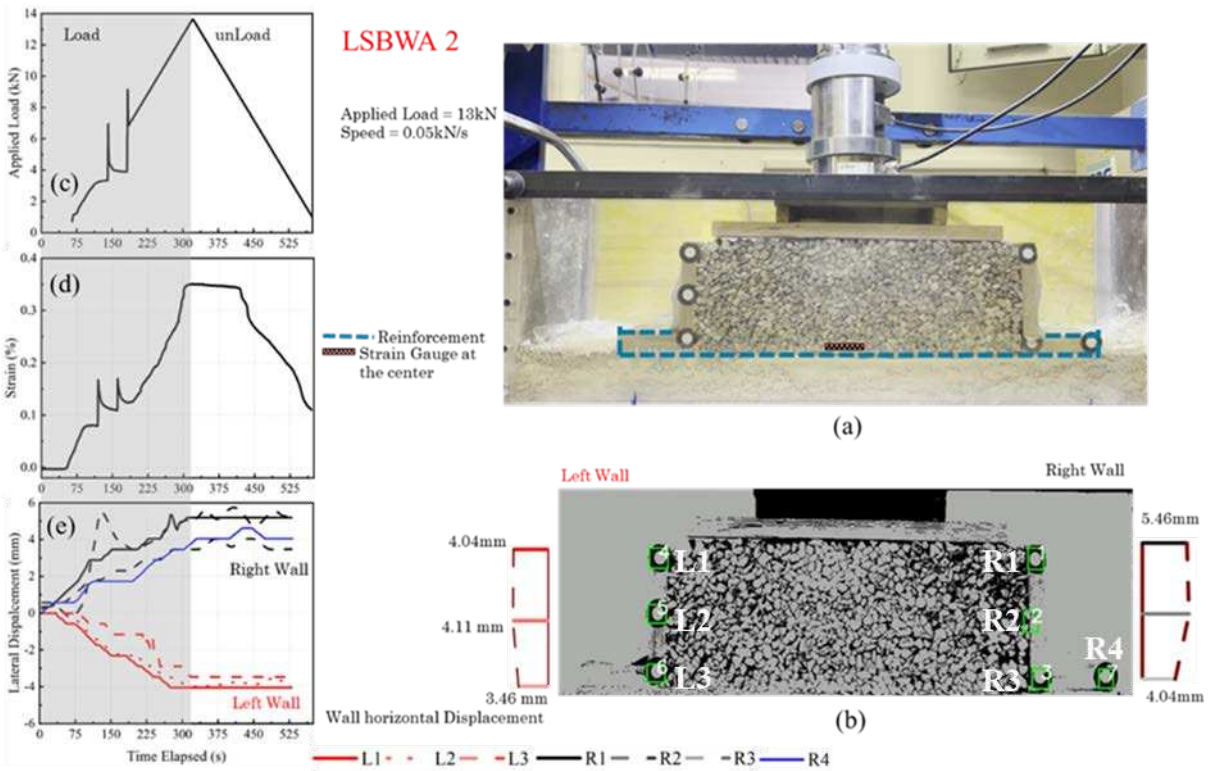

Figure 6. Test results of LSBWA 2 (a) Digital image during testing (b)) Processed image (c) Loading data (d) Strain, % vs. Time elapsed, seconds (e) Lateral displacement, mm vs. Time elapsed, seconds

4 DEVELOPMENT AND VALIDATION OF FINITE ELEMENT MODEL

A 3-dimensional finite element model (3D-FEM) was developed and validated with LSBWA-1 to configure the accurate interplay of BWA with reinforcements and corresponding load-deformation behavior. The BWA system was subjected to an external scaled load of 13 kN. The geometrical details of the developed finite element model were adopted similarly to the model scale tests. Table 1 summarizes input parameters used for gravel, sand, and reinforcement assumed from the properties of materials with similar behavior obtained from various sources of literature. The 3D-FEM simulations were carried out using the Abaqus implicit algorithm. Convergence issues resulting from excessive elemental distortions in the shearing zone were addressed by applying external load quasi-statically through this implicit algorithm. Accordingly, the loading rate for the numerical simulations was adopted to match the 1g model testing speed. The boundary conditions for the model domain were applied as follows: the base of the model was restrained from moving in the vertical (y) and horizontal directions (x, z). The vertical side boundary of the bottom soil was restrained in horizontal directions (x, z). The vertical side boundary of the BWA was not restrained to measure the lateral displacements. The front boundaries or lateral sides were restrained in one horizontal direction (z). It should be noted that the mesh size influences the accuracy of the solutions in finite element simulations. In this regard, a finer mesh size of 0.02m x 0.02m x 0.02m was considered in all directions. The illustrations of the model dimensions, finite element mesh, and boundary conditions adopted in the numerical simulations are shown in Fig. 7. The soil, ballast wall, and gravel continuum used for the foundation soil were discretized considering linear hexahedral elements with reduced integration (C3D8R). The embedded reinforcements were discretized with 4-noded membrane elements, with reduced integration (M3D4R). The thickness of the geogrid in the experimental model is 0.001 mm. The reinforcement used in the 1g reduced model tests is stiffer foil material. The gravel fill and bottom sand behavior was adopted based on Drucker-Prager yield criteria considering elasto-plastic behavior. The strategy applied for the soil-geogrid interface model is designed to capture both normal and tangential behavior at the contact. The sand-geogrid efficiency factor or interface friction coefficient was assumed as $\mu = 0.8$.

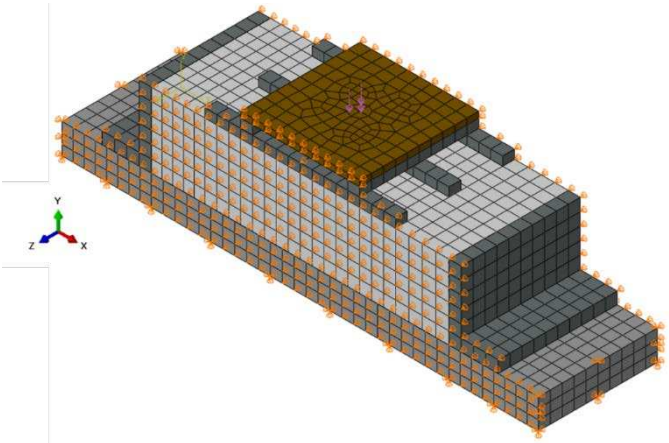

Figure 7. Developed 3D-FEM with meshing and boundary conditions.

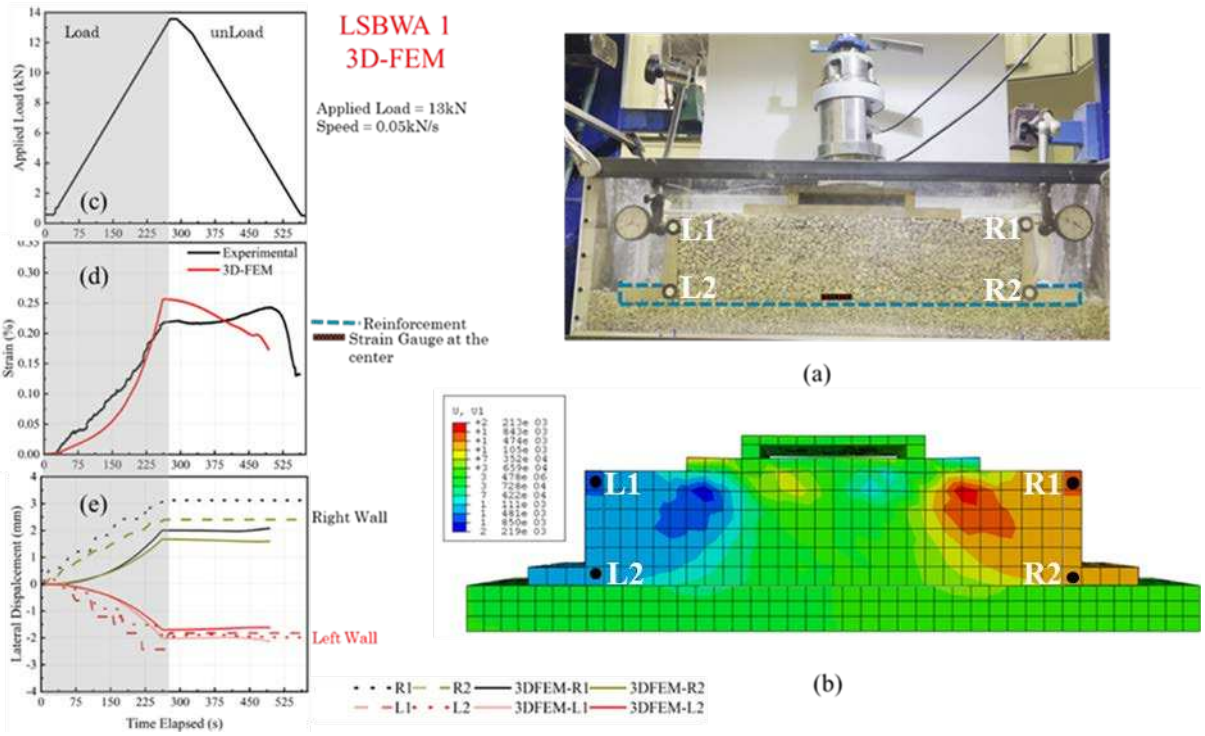

Figure 8. Results of numerical and experimental validation of LSBWA 1 (a) Digital image during at load 13kN (b) Horizontal displacement contour from 3D-FEM at load 13kN (c) Loading data (d) Strain, % vs. Time elapsed, seconds (e) Lateral displacement, mm vs. Time elapsed, seconds

Figs. 8(a) & (b) shows the image of the experimental model and horizontal displacement contour from 3D-FEM simulations for LSBWA 1. Fig. 8(d) presents strains of reinforcement obtained from these experimental and numerical simulations, which indicate a similar trend. The lateral displacement profile depicted in Figs. 8(e) showed a similar deformation behavior obtained from the experimental simulations for LASBWA 1. Compared with experimental observations, lateral deformations indicate that the 3D finite element model can closely predict the stability of LSBWA. These results showed the developed 3D numerical model's applicability to simulate the responses of BWAs. Peak lateral displacements of wall and geogrid strains exhibit similarity between experimental and 3D-FEM results, as shown in Figs. 8(d) & (e). However, the unloading curve in 3D-FEM, illustrated in Fig. 8(d), follows a descent, indicating the elastic nature of the reinforcement in use. In actuality, the considered reinforcement displays elasto-plastic behavior. Thus, further investigations will be carried out to establish the constitutive behavior of the reinforcement. Additionally, given the larger domains in the subsequent parametric analysis for field scale, a mesh convergence study is currently underway to reduce the substantial computational time.

5 CONCLUSIONS

The BWA system is a valuable alternative to conventional ballasted embankments subjected to various external loads. The end-to-end reinforcement connections at the bottom connect the BWA, significantly influencing its deformation response and ultimately addressing the confinement issues. A series of reduced-scale 1g physical tests and finite element simulations were performed to identify the critical issues of these modified tracks with LSBWA that require special attention in their design considerations. The results of the developed finite element model were benchmarked with the experimental findings. The results demonstrate that finite element analysis with a standard Mohr-Coulomb material model for ballast materials can reproduce reliable lateral deformation behavior with adequate finer meshing. The key findings from this study include the following:

a) The positive reinforcement effect is observed for these LSBWA systems, and the stability of the wall depends upon the stiffness of the reinforcement.

b) The observation from these initial tests indicates that BWA lateral deformation behavior concerning applied loads is instrumental in deciding the design parameters of reinforcement, such as reinforcement length, reinforcement stiffness, wall thickness, toe length, and various shapes of BWA.

c) The 3D-FEM is validated with the experimental results, which will be used for optimizing the design parameters by analyzing several probable scenarios

d) Further, this research is concentrated on evaluating the behavior of different shapes of BWAs and reinforcement connections when subjected to static and dynamic loads.

e) The reinforcing mechanism is the governing factor in holding the BWA in these ballasted track systems. This mechanism varies with the shape of the ballasted wall and connections to reinforcement, although the shape effect and effect of reinforcement connections are not presented here.

ACKNOWLEDGEMENTS

The authors are grateful for the financial support provided by LIAISON (HORIZON-CL5-2022-D6-02-06) and by the Ministry of Higher Education, Science and Technology of the Republic of Slovenia - and The Slovenian Research Agency (ARRS) Programme group P2-0273 and Core funding Z1-1858.

REFERENCES

Aela, P., Jia, W.L. and Jing, G.Q. (2021) ‘Effect of ballast retaining walls on the lateral resistance of railway tracks’, Proceedings of the Institution of Mechanical Engineers, Part F: Journal of Rail and Rapid Transit, 235(4), pp. 416–424.

Biabani, M.M., Ngo, N.T. and Indraratna, B. (2016) ‘Performance evaluation of railway subballast stabilised with geocell based on pull-out testing’, Geotextiles and Geomembranes, 44(4), pp. 579–591.

EN 13450 (2013) Aggregates for railway ballast.

Gong, H. et al. (2019) ‘Direct shear properties of railway ballast mixed with tire derived aggregates: Experimental and numerical investigations’, Construction and Building Materials, 200, pp. 465–473.

Guo, Y. et al. (2022) ‘Railway ballast material selection and evaluation: A review’, Construction and Building Materials, 344, p. 128218.

Indraratna, B. et al. (2022) ‘The role of recycled rubber inclusions on increased confinement in track substructure’, Transportation Geotechnics, 36.

Indraratna, B., Biabani, M.M. and Nimbalkar, S. (2015) ‘Behavior of Geocell-Reinforced Subballast Subjected to Cyclic Loading in Plane-Strain Condition’, Journal of Geotechnical and Geoenvironmental Engineering, 141(1).

Indraratna, B., Ngo, N.T. and Rujikiatkamjorn, C. (2013) ‘Deformation of Coal Fouled Ballast Stabilized with Geogrid under Cyclic Load’, Journal of Geotechnical and Geoenvironmental Engineering, 139(8), pp. 1275–1289.

Indraratna, B., Sun, Q. and Grant, J. (2017) ‘Behaviour of subballast reinforced with used tyre and potential application in rail tracks’, Transportation Geotechnics, 12, pp. 26–36.

Leshchinsky, B. and Ling, H.I. (2013) ‘Numerical modeling of behavior of railway ballasted structure with geocell confinement’, Geotextiles and Geomembranes, 36, pp. 33–43.

Prasad, K.V.S. and Hussaini, S.K.K. (2022) ‘Review of different stabilization techniques adapted in ballasted tracks’, Construction and Building Materials, 340, p. 127747.

Sadeghi, J. and Askarinejad, H. (2009) ‘An investigation into the effects of track structural conditions on railway track geometry deviations’, Proceedings of the Institution of Mechanical Engineers, Part F: Journal of Rail and Rapid Transit, 223(4), pp. 415–425.

Sol-Sánchez, M., Moreno-Navarro, F. and Rubio-Gámez, M.C. (2014) ‘Viability of using end-of-life tire pads as under sleeper pads in railway’, Construction and Building Materials, 64, pp. 150–156.

Wood, D.M. (2004) ‘Geotechnical modelling’, Version 2., p. 488.